Neurocomputing 148 (2015) 561–568

Contents lists available at ScienceDirect

Neurocomputing

journal homepage: www.elsevier.com/locate/neucom

SAR complex image data compression based on quadtree and zerotree Coding in Discrete Wavelet Transform Domain: A Comparative Study

Xingsong Hou [a,*], Min Han [a], Chen Gong [b], Xueming Qian [a]

[a] School of Electronics and Information Engineering, Xi'an Jiaotong University, Xi'an, China
[b] Qualcomm Research, San Diego, CA, USA

ARTICLE INFO

Article history:
Received 28 January 2014
Received in revised form
10 April 2014
Accepted 2 July 2014
Communicated by: M. Wang
Available online 22 July 2014

Keywords:
Quadtree
SAR complex image data compression
Zerotree

ABSTRACT

A SAR complex image data compression algorithm based on quadtree coding (QC) in discrete wavelet transform (DWT) domain (QC-DWT) is proposed. We show that QC-DWT achieves the best performance for SAR complex image compression. Besides this, in this work, we observed a novel phenomenon that QC-DWT outperforms the zerotree based wavelet coding algorithms, e.g., Consultative Committee for Space Data Systems-Image Data Compression (CCSDS-IDC) and Set Partitioning in Hierarchical Trees algorithm (SPIHT) for SAR complex image data, and there exists deficiency of CCSDS-IDC for SAR complex image data compression. This is because the DWT coefficients of SAR complex image data always have intrascale clustering characteristic and no interscale attenuation characteristic, which is different from that of SAR amplitude images and other optical images.

1. Introduction

Synthetic aperture radar (SAR) has been widely used in remote sensing for both civil and military applications. Unlike optical image, SAR image data is always complex. For example, interference SAR can use the phase difference of two SAR complex image data to obtain the elevation information and has been widely applied in the environmental monitoring, mapping, and other fields [1]. However, vast amounts of SAR complex image data require transmission and storage resources, which raise the needs for efficient SAR complex image data compression.

DWT based image coding is the representative coding algorithm for SAR image data compression [2–4]. Image wavelet coefficients often exhibit attenuation and clustering characteristics [5]. Accordingly, two types of image coding algorithms are popular. The first mainly uses the attenuation characteristic, such as Set Partitioning in Hierarchical Trees algorithm (SPIHT) [6] and Consultative Committee for Space Data Systems-Image Data Compression (CCSDS-IDC) [7], which have already been used for SAR amplitude image data compression [4,7]. The second mainly uses the clustering characteristic, such as quadtree coding (QC) [8], which has also been used for SAR amplitude image compression [3]. The wavelet image coding algorithms exploiting these two characteristics show similar performance for SAR amplitude and optical images [7,9].

For SAR complex image data compression, CCSDS-IDC based on DWT (DWT-CCSDS), which exploits the wavelet attenuation characteristic, exhibits poor performance for SAR complex image data due to the lack of interscale attenuation property [2]. Based on this, DLWT-CCSDS which combines directional lifting wavelet transform (DLWT) with the zerotree based bit plane encode (BPE) algorithm of CCSDS-IDC is proposed. It outperforms the DWT-CCSDS because DLWT can concentrate the energy to low frequency, which is beneficial to zerotree coding. However, for the test images, the K-term nonlinear approximation of DLWT is not as good as that of DWT [2], which limits further performance improvement based on DLWT for SAR complex image data. On the other hand, although QC, which exploits the intrascale clustering property, has already been used for SAR amplitude image compression [3], it has not been used for SAR complex image data compression.

In this work, to achieve a SAR complex image data compression algorithm with high performance, we first analyze the DWT coefficients' intrascale and interscale characteristics of SAR complex image data in Section 2. Then a QC based SAR complex image data compression algorithm is proposed in Section 3. Experimental results are shown in Section 4. Section 5 concludes this paper.

2. DWT coefficients characteristics analysis of SAR complex image data

The SAR complex image data used in this work consists of 1024×1024 pixel with 16-bit per pixel, which is downloaded from the U.S. Sandia National Laboratories [10]. Fig. 1 shows the real-parts of

* Corresponding author.
E-mail address: houxs@mail.xjtu.edu.cn (X. Hou).

http://dx.doi.org/10.1016/j.neucom.2014.07.007
0925-2312/

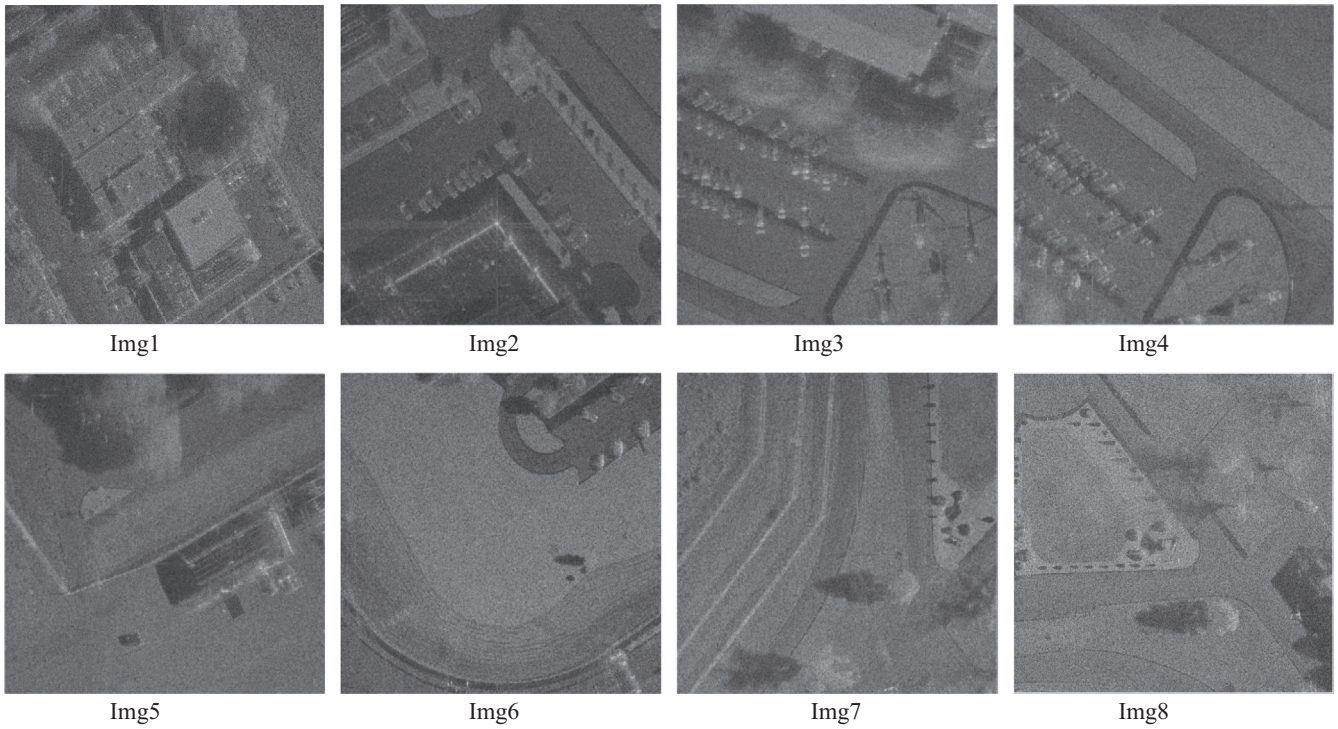

Fig. 1. Real-parts of the testing SAR complex image data.

the SAR complex images, and the imaginary-parts and amplitude images are similar to the real-parts and thus are omitted. Here, we adopt three-level 9/7 biorthogonal DWT and analyze the properties of SAR complex image data wavelet coefficients from two aspects: intrascale and interscale correlations.

2.1. Intrascale clustering characteristic of DWT coefficients

Fig. 2 shows the position distribution of significant DWT coefficients for the real-part (the imaginary-part is similar and omitted) and amplitude of Img2 with three levels DWT decomposition where the largest 10% and 30% magnitude of DWT coefficients are preserved as significant DWT coefficients. The amplitude images are used as a comparison. Significant coefficients are shown in white and other coefficients are shown in black. It is seen that DWT coefficients exhibit obvious intrascale clustering along contours or in textured regions both for SAR complex image data and amplitude image. Moreover, the DWT coefficients clustering of SAR complex images are mainly distributed on small scale, while, the clustering for amplitude images concentrates on DC and large scale.

When the largest 10% and 30% magnitude of DWT coefficients are reserved, Table 1 shows the fractions of insignificant DWT coefficient blocks of SAR complex image data in different block sizes. There are plenty of 2×2 and 4×4 insignificant DWT coefficient blocks. For example, there is an average 76.2% insignificant 2×2 block of all 2×2 blocks when keep the largest 10% magnitude of DWT coefficients. In the encoding procedure, these insignificant DWT coefficient blocks can be encoded as one unit, which saves many coding bits. So, more insignificant DWT coefficient blocks there are, better coding performance it will be.

2.2. Interscale attenuations characteristic of DWT coefficients

Fig. 3 gives the average DWT coefficients amplitude distribution of eight SAR complex images and amplitude images, where DWT coefficients are scanned by the order of DC—HL3—LH3—HH3—HL2—LH2—HH2—HL1—LH1—HH1 as shown in Fig. 4. It is seen that they have opposite distribution. For SAR complex image data, the large-amplitude DWT coefficients are mainly distributed on small scale. While, the large-amplitude DWT coefficients of SAR amplitude images are mainly distributed on DC and large scale and amplitude attenuation is clear.

To quantify the attenuation property, the attenuation index (AI): $\mathrm{AI}=n_s/N_s$ is defined, where n_s is the number of attenuated wavelet coefficients on scale s, and N_s is the number of wavelet coefficients on scale s. Here the attenuated wavelet coefficient on small scale is the one that is less than the corresponding wavelet coefficients on the nearest big scale. Table 2 shows the attenuation of wavelet coefficients on each scale for SAR complex image data and amplitude images. It can be seen that the average attenuation index of SAR complex images is 0.2443 and 0.2208 on scale 1 and scale 2, which are much less than that of SAR amplitude images.

The wavelet coefficient amplitude often decreases when the scale decreases; but when the signal has a high-frequency oscillation, the attenuation property across scales is not obvious [11]. Fig. 5 shows the 128nd row data of real-part (the imaginary-part is similar and omitted) and amplitude images of Img2. There exists strong oscillation for the SAR complex image data, which leads to large-amplitude coefficients in small scales and the attenuation of wavelet coefficients decreased from large scale to small scale. However, the amplitude of Img2 has no strong oscillation compared with the SAR complex image data.

For zerotree based coding algorithm, such as CCSDS-IDC, SPIHT, there are different coding symbol lengths for coefficients distributed in different scales [2,6,7], which means fewer bits are needed for the significant DWT coefficient in the parent. The zerotree based wavelet coding is most suitable for images with attenuation property from large scale to small scale. However, the significant DWT coefficients of SAR complex image data are mainly concentrated on small scale grandchildren coefficients, which means that CCSDS-IDC [7], SPIHT [6] may not be suitable for SAR complex image data. QC is a good choice because it utilizes the clustering property of significant coefficients.

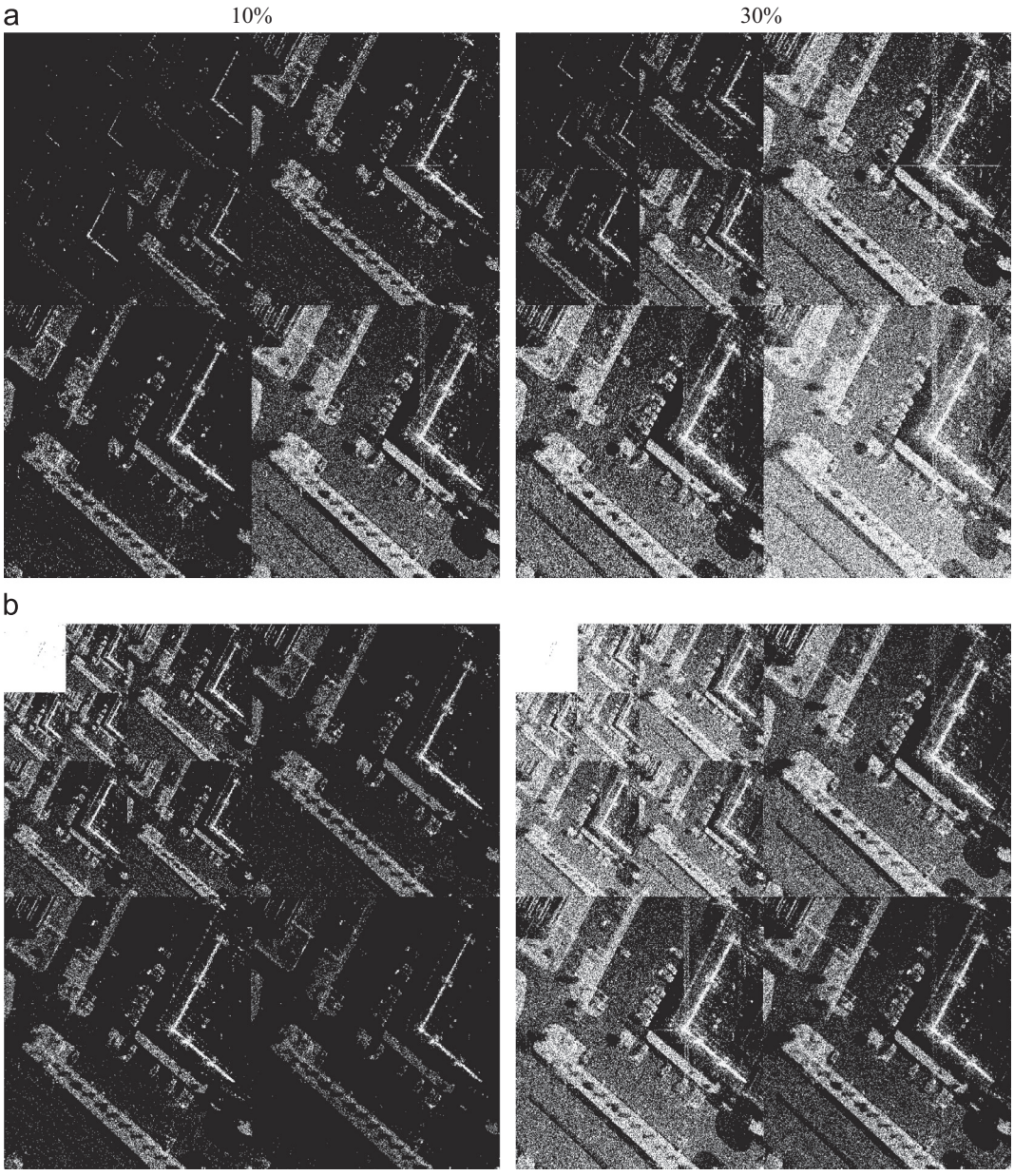

Fig. 2. The position distribution of significant DWT coefficients. (a) Real-part image of Img2. (b) Amplitude image of Img2.

Table 1
The amount proportion of insignificant DWT coefficient blocks.

Images	10%					30%				
	2×2	4×4	8×8	16×16	32×32	2×2	4×4	8×8	16×16	32×32
Img1	0.773	0.579	0.321	0.088	0.045	0.452	0.246	0.088	0.022	0.009
Img2	0.777	0.594	0.325	0.076	0.032	0.443	0.226	0.079	0.023	0.010
Img3	0.779	0.614	0.372	0.114	0.045	0.456	0.257	0.097	0.025	0.009
Img4	0.756	0.551	0.313	0.123	0.077	0.425	0.210	0.094	0.040	0.008
Img5	0.756	0.553	0.322	0.322	0.149	0.435	0.257	0.126	0.042	0.024
Img6	0.749	0.544	0.337	0.183	0.158	0.431	0.247	0.136	0.067	0.048
Img7	0.756	0.556	0.340	0.232	0.103	0.421	0.223	0.116	0.052	0.042
Img8	0.753	0.557	0.332	0.171	0.132	0.423	0.229	0.130	0.056	0.043
Average	0.762	0.568	0.332	0.163	0.092	0.435	0.236	0.108	0.040	0.024

3. Quadtree coding for SAR complex image data

Since the wavelet coefficients exhibit clustering property, we adopt QC to encode SAR complex image data. The basic idea is to continuously divide the image into four parts, and check the significance of each part. Before giving the QC, we define some variables: (1) *T*: quantization level; (2) *LSP*: the list of significant coefficients which is used to store the coordinate of significant

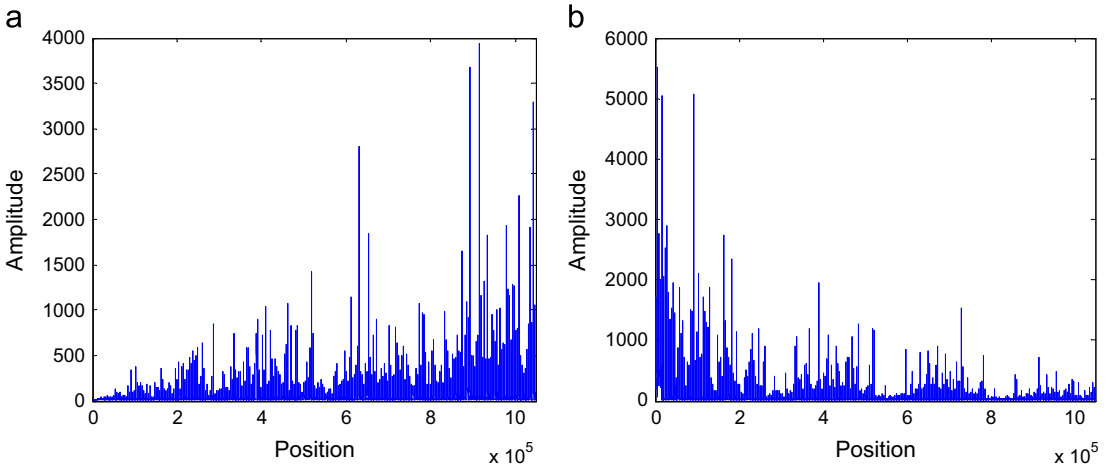

Fig. 3. Average DWT coefficients amplitude distribution. (a) SAR complex image (b) SAR amplitude image.

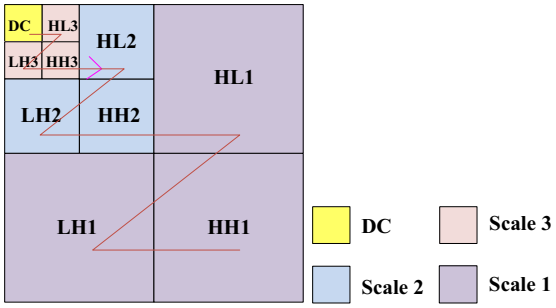

Fig. 4. DWT subbands and scanning order.

Table 2
The attenuation index on each scale.

Images	SAR complex images		SAR amplitude images	
	Scale1	Scale2	Scale1	Scale2
Img1	0.2578	0.2413	0.6697	0.6140
Img2	0.2512	0.2396	0.6626	0.5933
Img3	0.2454	0.2298	0.6599	0.5863
Img4	0.2465	0.2127	0.6591	0.5819
Img5	0.2408	0.2144	0.6578	0.5676
Img6	0.2394	0.2026	0.6616	0.5721
Img7	0.2368	0.2128	0.6640	0.5755
Img8	0.2367	0.2132	0.6649	0.5766
Average	0.2443	0.2208	0.6624	0.5834

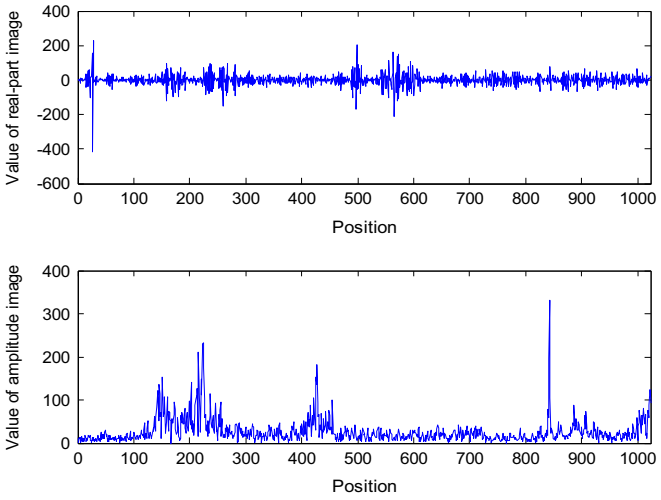

Fig. 5. The 128th row data of real-part image and amplitude image of Img2.

coefficients; (3) *LIB*: the list used to store the up and bottom coordinates of the significant blocks; (4) $s_\tau(k,T)$: the significance of block k compared with quantization level T (τ refers to the coordinate set of wavelet coefficients in block k); use

$$s_\tau(k,T)=\begin{cases}1, & \max\limits_{(i,j)\in\tau}\{|c(i,j)|\}\geq T\\ 0, & \text{otherwise}\end{cases}$$

to represent the significance of the block k.

QC consists of five steps: initialization, quadtree splitting, coefficient refining, updating and arithmetic coding. In the main quadtree split step, at a quantization level T, for each block k in *LSP* do: Output $s_\tau(k,T)$; If $s_\tau(k,T)=1$, divide block k into four parts and judge whether it is the last partition or not. If there are only four DWT coefficients, output the significance and sign of the DWT coefficients and move its coordinate to *LSP*. Otherwise, make coordinates of the four parts as new nodes and add them to the *LIB*. Then, remove block k from *LIB*. At the last step, output the above binary bits to the arithmetic coding without context modeling.

The decoding algorithm is similar to the encoding algorithm and thus omitted here. The efficiency of QC for SAR complex data is given in the following section.

4. Experimental results and analysis

4.1. Coding performance of quadtree and zerotree coding for SAR complex image data

We use amplitude peak signal-to-noise ratio (PSNR) and mean phase error (MPE) [2] to measure the performance of coding algorithms for SAR complex image data. Here, the real- and imaginary-parts of SAR complex image data are encoded with equal rate separately. Moreover, we adopt three-level 9/7 biorthogonal DWT decomposition in all experiments. QC based on DWT (DWT-QC) and zerotree coding algorithm: DWT-CCSDS are used for comparison. Since SPIHT algorithm shows similar performance to that of DWT-CCSDS [2], we do not compare it with DWT-QC. As DLWT aggregates the energy of coefficients to low frequency for SAR complex image, DLWT-CCSDS outperforms DWT-CCSDS [2]. In this work, DLWT-CCSDS and QC based on DLWT (DLWT-QC) are also shown to compare the performance of QC and zerotree coding algorithm in DLWT domain.

Tables 3 and 4 show amplitude PSNR and MPE of these coding algorithms at the rates 4, 2 and 1 bpp (bit per pixel), respectively. It is

Table 3
Comparisons of coding performance in amplitude PSNR (dB).

Imgs	4 bpp				2 bpp				1 bpp			
	DWT-QC	DWT-CCSDS	DLWT-CCSDS	DLWT-QC	DWT-QC	DWT-CCSDS	DLWT-CCSDS	DLWT-QC	DWT-QC	DWT-CCSDS	DLWT-CCSDS	DLWT-QC
Img1	86.30	82.68	84.05	84.33	75.11	71.95	73.15	73.43	69.22	66.32	67.54	67.98
Img2	91.05	87.54	88.54	89.38	80.31	76.62	77.43	78.15	74.23	71.24	72.16	72.83
Img3	82.85	78.98	79.87	80.20	71.15	68.69	68.89	72.34	65.05	63.45	63.47	67.55
Img4	86.76	82.88	84.13	84.55	75.37	72.21	73.40	73.85	69.68	67.27	68.43	68.71
Img5	88.86	84.46	85.78	86.53	76.98	74.51	74.61	75.12	71.00	69.25	69.33	69.74
Img6	90.34	86.98	87.65	88.53	78.75	75.43	76.09	76.90	72.91	70.13	70.88	71.58
Img7	87.82	84.00	84.92	85.48	76.31	73.65	74.16	74.56	70.59	68.96	69.10	69.52
Img8	82.05	78.16	78.96	79.65	70.28	67.52	68.00	68.43	64.60	62.81	62.84	63.31

Table 4
Comparisons of coding performance in MPE (Radian).

Imgs	4 bpp				2 bpp				1 bpp			
	DWT-QC	DWT-CCSDS	DLWT-CCSDS	DLWT-QC	DWT-QC	DWT-CCSDS	DLWT-CCSDS	DLWT-QC	DWT-QC	DWT-CCSDS	DLWT-CCSDS	DLWT-QC
Img1	0.231	0.309	0.258	0.267	0.733	0.917	0.829	0.835	1.189	1.468	1.322	1.286
Img2	0.216	0.326	0.276	0.238	0.701	0.970	0.856	0.808	1.171	1.496	1.368	1.318
Img3	0.197	0.294	0.281	0.279	0.664	0.931	0.861	0.469	1.131	1.418	1.349	0.647
Img4	0.188	0.262	0.226	0.229	0.629	0.829	0.761	0.753	1.112	1.374	1.262	1.250
Img5	0.191	0.283	0.266	0.265	0.621	0.848	0.809	0.782	1.030	1.342	1.280	1.225
Img6	0.190	0.288	0.262	0.246	0.601	0.887	0.781	0.759	1.033	1.401	1.253	1.201
Img7	0.178	0.245	0.228	0.230	0.594	0.790	0.762	0.749	1.046	1.330	1.230	1.216
Img8	0.192	0.261	0.247	0.246	0.595	0.789	0.783	0.751	1.006	1.300	1.259	1.207

seen that DWT-QC shows the best performance among all schemes. Compared with DWT-CCSDS, DWT-QC improves PSNR up to 4.4, 3.69, 2.99 dB at 4, 2 and 1 bpp, and increases up to 0.110, 0.286, and 0.368 reductions at 4, 2 and 1 bpp in MPE, respectively. DWT-QC also outperforms DLWT-CCSDS by achieving PSNR improvements up to 3.09, 2.88, 2.07 dB and MPE reduction up to 0.084, 0.197, 0.253 at 4, 2, 1 bpp, respectively. It is seen that DWT-QC still outperforms DLWT-QC because the K-term nonlinear approximation of DLWT is not good as that of DWT [2]. The coding algorithm exploiting clustering characteristic outperforms coding algorithm using attenuation characteristic both in DWT and DLWT domain for SAR complex image data compression.

Fig. 6 shows the reconstructed amplitude images of SAR complex image data at rate of 2 bpp for DWT-QC, DWT-CCSDS, DLWT-CCSDS and DLWT-QC to compare the visual quality of coding algorithms. It can be seen that DWT-QC achieves the best visual quality.

4.2. Significance coding analysis of quadtree and zerotree coding for SAR complex image data

Here we use the number of significance coding bits on each bit plane to explain the advantage of QC used for SAR complex image data compression, where significance coding bits refer to bits used to encode the significance of wavelet coefficients, like as the bits spending on $s_\tau(k,T)$ for QC and *Type P*, *Tran B*, *Tran D*, *Type C*, *Tran G*, *Tran H* and *Type H* for CCSDS-IDC. Here *Types P*, *Type C and Type H* denote the significance of parent, children, and grandchildren coefficients, respectively; *Tran B and Tran D* denote the significance of the set of descendant coefficients in a block and families, respectively; *Tran G* denotes the significance of the set of grandchildren coefficients and *Tran H* denotes the significance of the further partition set of grandchildren coefficients in a family [7]. Fig. 7 shows the average significance coding bits on each bit plane for the eight real-parts of SAR complex image data. It is seen that DWT-QC shows the fewest significance coding bit clearly from bit plane 4 to bit plane 10. At the same rate, QC can encode more information of DWT coefficients due to the saving bits on bit plane 4 to 10. Compared with the zerotree coding algorithms using attenuation characteristic, QC exploiting clustering characteristic is more efficient for SAR complex image data coding.

4.3. Coding performance of SAR amplitude images

Table 5 gives PSNR of coding algorithms for SAR amplitude images. QC still shows comparable performance for SAR amplitude images as that for other schemes. For SAR amplitude images coding, exploited clustering characteristic or attenuation characteristic has no significant difference, which is different from that of the SAR complex image data. This is due to the wavelet coefficients of SAR amplitude images exhibits clustering characteristic and attenuation characteristic.

5. Conclusions

In this work, we have proposed DWT-QC for SAR complex image data compression. Experimental results have shown that, for SAR complex image data, DWT-QC can achieve higher performance than zerotree coding algorithms. For SAR amplitude image data, QC achieves similar performance compared with zerotree coding algorithms. We also find CCSDS-IDC suffers low efficiency for SAR complex image data compression. This is because, for SAR complex image data, clustering characteristic exists in wavelet coefficients, while attenuation characteristic is lost.

This study has also clarified an inaccurate common sense: the wavelet image coding algorithms exploiting clustering property and attenuation property have a similar performance [7,9]. Since the attenuation property may lose due to lack of the smooth constraint and the clustering property of image geometrical structure always exists, for designing image coding algorithm with DWT, considering clustering property may be the first choice to

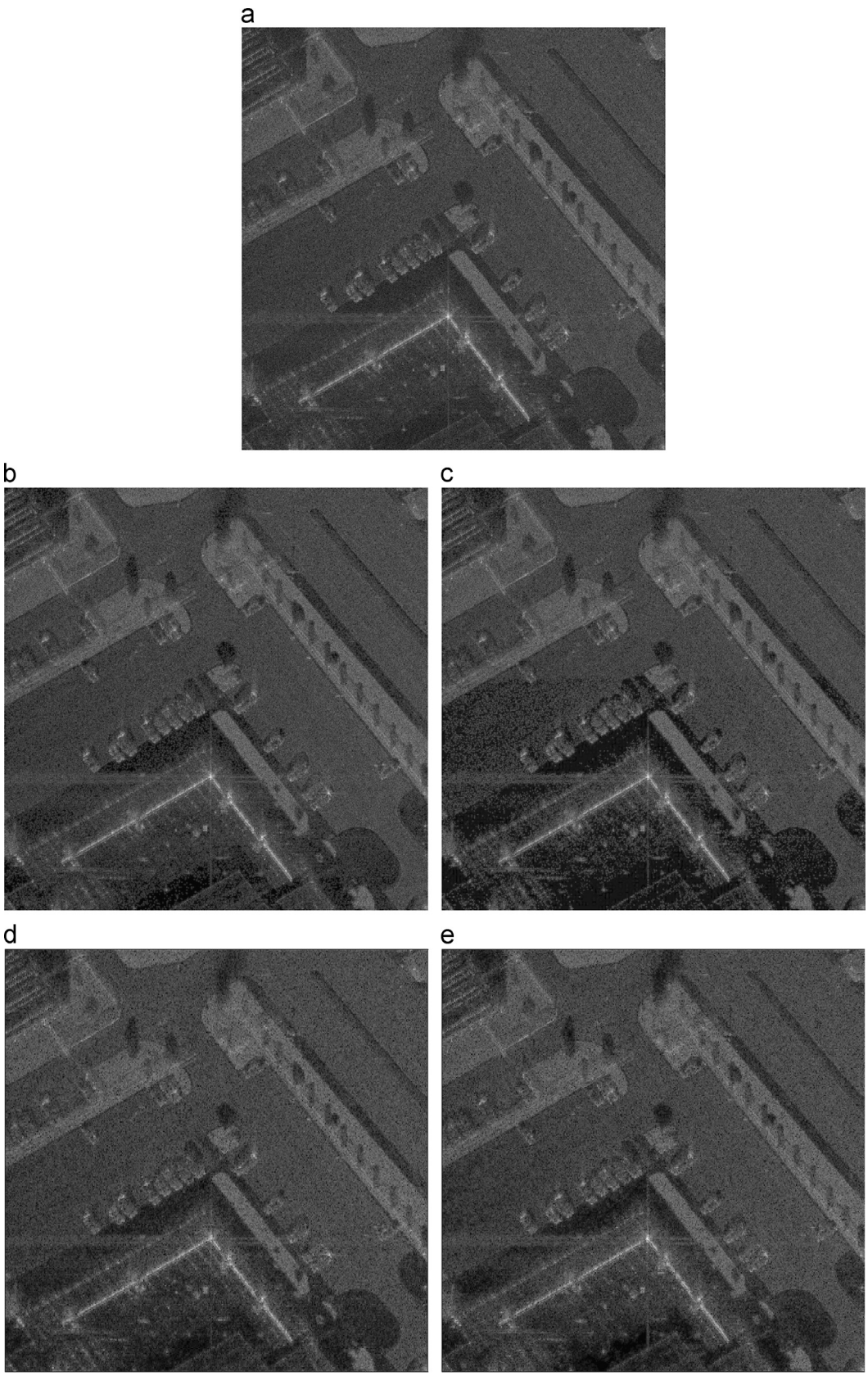

Fig. 6. Visual comparison of amplitude of Img2. (a) Original amplitude of Img2. (b) DWT-QC at 2 bpp (c) DWT-CCSDS at 2 bpp. (d) DLWT-CCSDS at 2 bpp (e) DLWT-QC at 2 bpp.

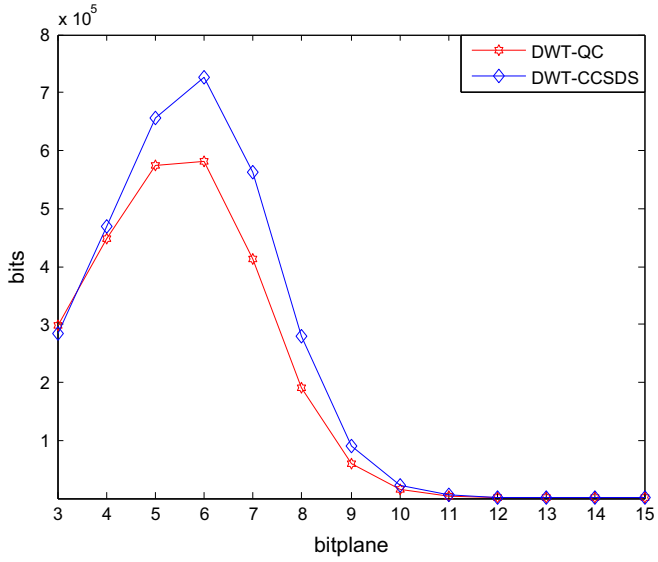

Fig. 7. Significance coding bits on each bit plane.

Table 5
Comparisons of coding performance for SAR amplitude image in PSNR (dB).

Imgs	4 bpp				2 bpp				1 bpp			
	DWT-QC	DWT-CCSDS	DLWT-CCSDS	DLWT-QC	DWT-QC	DWT-CCSDS	DLWT-CCSDS	DLWT-QC	DWT-QC	DWT-CCSDS	DLWT-CCSDS	DLWT-QC
Img1	87.36	87.47	87.45	87.39	76.19	75.91	75.97	76.27	70.73	70.50	70.55	70.82
Img2	92.12	92.28	92.35	92.13	81.18	81.00	80.97	81.17	76.10	75.88	75.96	76.19
Img3	83.90	84.01	83.99	83.90	72.63	72.82	72.82	72.31	67.23	67.27	67.27	67.25
Img4	87.73	87.66	87.63	87.75	76.38	76.04	76.13	76.48	71.49	71.15	71.25	71.59
Img5	89.79	89.82	89.83	89.80	78.20	78.12	78.25	78.30	72.85	72.81	72.92	72.97
Img6	91.16	91.16	91.18	91.18	79.96	79.94	79.97	80.02	74.72	74.61	74.69	74.83
Img7	89.01	88.77	88.75	89.05	77.33	77.14	77.23	77.43	72.40	72.29	72.39	72.52
Img8	83.37	83.19	83.17	83.38	71.29	71.15	71.25	71.40	66.27	66.16	66.27	66.40

cover a wider range of images compared with considering attenuation property.

Acknowledgements

This work was supported by National Natural Science Foundation of China (no. 61373113) and the Fundamental Research for the Central University (no. xjj2012023).

References

[1] P.A. Rosen, S. Hensley, I.R. Jourhin, F.K. Li, S.N.Madsen, E. Rodríguez, R.M. Goldstein, Synthetic aperture radar interferometry, in: Proc. IEEE, Mar. 2000, 88, 3, 333–382.
[2] X.S. Hou, J. Yang, G.F. Jiang, X.M. Qian, Complex SAR image compression based on directional lifting wavelet transform with high clustering capability, IEEE Trans. Geosci. Remote Sens. 51 (1) (2013) 527–538.
[3] X.S. Hou, G.Z. Liu, Y.Y. Zou, SAR image data compression using wavelet packet transform and universal-trellis coded quantization, IEEE Trans. Geosci. Remote Sens. 42 (11) (2004) 2632–2641.
[4] Z. Zeng, I.G. Cumming, SAR image data compression using a tree-structured wavelet transform, IEEE Trans. Geosci. Remote Sens. 39 (3) (2001) 546–552.
[5] M.S. Crouse, R.D. Nowak, R.G. Baraniuk, Wavelet-based statistical signal processing using hidden Markov models, IEEE Trans. Signal Proces. 46 (4) (1998) 886–902.
[6] S. Amir, A.P. Pearlman, A new fast and efficient image codec based on set partitioning in hierarchical trees, IEEE Trans. Circuits Syst. Video Technol. 6 (3) (1996) 243–250.
[7] ⟨http://public.ccsds.org/publications/archive/120 × 1g1e2.pdf⟩.
[8] A. Menteanu, J. cornelis, G. Van Der Auwera, P. Crustea, Wavelet image compression-the quadtree coding approach, IEEE Trans. Inf. Technol. Biomed. 3 (3) (1999) 176–185.
[9] B.A. Banister, T.R. Fischer, Quadtree classification and TCQ image coding, IEEE Trans. Circuits Syst. Video Technol. 11 (1) (2001) 3–8.
[10] ⟨http://www.sandia.gov/radar/sar-data.html⟩.
[11] S. Mallat, A Wavelet Tour of Signal Processing: The Sparse Way, third ed., Academic, Orlando, 2008.

Xingsong Hou received the Ph.D. degree from Xi'an Jiaotong University, Xi'an, China, in 2005. Now, he is an Associate Professor with the School of Electronics and Information Engineering, Xi'an Jiaotong University. His research interests include video/image coding, wavelet analysis, sparse representation, sparse representation and compressive sensing, and radar signal processing. During October 2010–2011, he was a Visiting Scholar at Columbia University, New York, USA.

Min Han received the B.S. degree from Xi'an University of Post & Telecommunications in 2011. Now she is pursuing her M.S. degree from Xi'an Jiaotong University, Xi'an, China. Her research interest is image coding.

Chen Gong received the B.S. degree in electrical engineering and mathematics (minor) from Shanghai Jiaotong University, Shanghai, China in 2005, and M.S. degree in electrical engineering from Tsinghua University, Beijing, China in 2008. He received the Ph.D degree in Electrical Engineering from Columbia University in May 2012. Now he is working in Qualcomm Inc., San Diego, Californina, USA. His research interests are in the area of channel coding and modulation techniques for wireless communications and signal processing.

Xueming Qian received the B.S. and M.S. degrees from the Xi'an University of Technology, Xi'an, China, in 1999 and 2004, respectively, and the Ph.D. degree from Xi'an Jiaotong University, Xi'an, China, in 2008. He was awarded a Microsoft fellowship in 2006. From 1999 to 2001. He was an Assistant Engineer at Shannxi Daily. From 2008 until now, he has been a Faculty Member with the School of Electronics and Information Engineering, Xi'an Jiaotong University. He was a Visiting Scholar at Microsoft Research Asia from August 2010 to March 2011. His research interests include video/image analysis, indexing, and retrieval.